Large-scale solar cycle features of solar photospheric magnetic field [⋆]

W.B. Song [*]

State Key Laboratory for Space Weather, Center for Space Science and Applied Research, Chinese Academy of Sciences, Beijing 100080, China

Abstract

It is well accepted that the solar cycle originates from a magnetohydrodynamics dynamo deep inside the Sun. Many dynamo models have long been proposed based on a lot of observational constraints. In this paper, using 342 NSO/Kitt Peak solar synoptic charts we study the solar cycle phases in different solar latitudinal zones to set further constraints. Our results can be summarized as follows. (1) The variability of solar polar regions' area has a correlation with total unsigned magnetic flux in advance of 5 years. (2) The high-latitude region mainly appears unipolar in the whole solar cycle and its flux peak time lags sunspot cycle for 3 years. (3) For the activity belt, it is not surprised that its phase be the same as sunspot's. (4) The flux peak time of the low-latitude region shifts forward with an average gradient of 32.2 *day/deg*. These typical characteristics may provide some hints for constructing an actual solar dynamo.

Key words: solar cycle, photosphere, solar magnetic field

1 Introduction

Dynamo theory recognized to reproduce the solar cycle has continuously been a hot topic in solar physics since fifty years ago (e.g., Parker, 1955). For example, in the classical $\alpha - \Omega$ turbulent dynamo, two basic processes are involved. The first one is Ω-effect which shears pre-existing poloidal fields by differential rotation to produce a relatively strong toroidal fields; the second one is

⋆ This work is jointly supported by the National Natural Science Foundation of China (40604019) and the 973 project under grant 2006CB806304.
* W.B. Song
Email address: wbsong@spaceweather.ac.cn (W.B. Song).

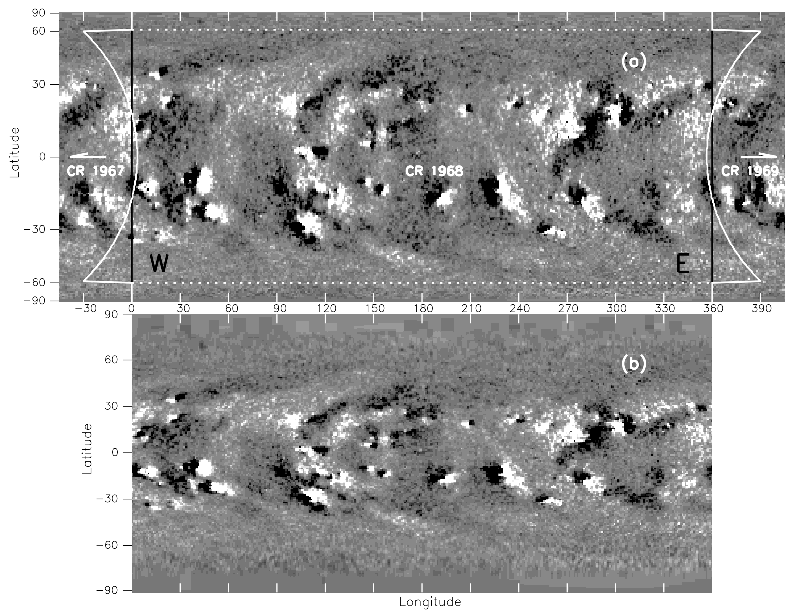

Fig. 1. (a) Three connected NSO/Kitt Peak magnetic synoptic charts of CR1967-1969. Two solid white lines outline the real region corresponding to full solar disk. (b) The newly constructed synoptic chart with a grid of 360 equal steps in longitude by 180 equal steps in latitude.

α-effect which lifts and twists toroidal flux tubes to regenerate poloidal fields (Parker, 2001). Nowadays many dynamo models have been developed in which the major observational constraints come from the sunspot behavior, such as butterfly diagram, differential rotation, Hale magnetic solar cycles, and so on. In addition, based on a deep meridional flow found in both hemispheres, some flux-transport dynamo models are constructed (see Dikpati, 2005). Li et al. (2005) design a flux tube dynamo model by use of solar internal rotation on the assumption of a downflow effect under photosphere. In this paper, using solar magnetic synoptic charts we investigate the large-scale solar cycle features in different latitudinal strips and expect such information can provide helps for constructing a more reliable dynamo.

2 Database

In this paper we use NSO/Kitt Peak magnetic synoptic charts during Carrington Rotations (CRs) 1666-2007 as our database which show the distribution of solar radial magnetic fields. Each magnetogram covers one CR and has a grid of 360 equal steps in longitude by 180 equal steps in sine latitude. First, as shown in figure 1a, we connect all charts in time order (Stenflo & Güdel 1988) and outline the real region corresponding to full solar disk. In the range of latitude $|\theta| \leq 60°$, two concave sidelines are due to differential rotation (Song & Wang 2005). Meanwhile, for the polar regions (PRs) where $|\theta| > 60°$,

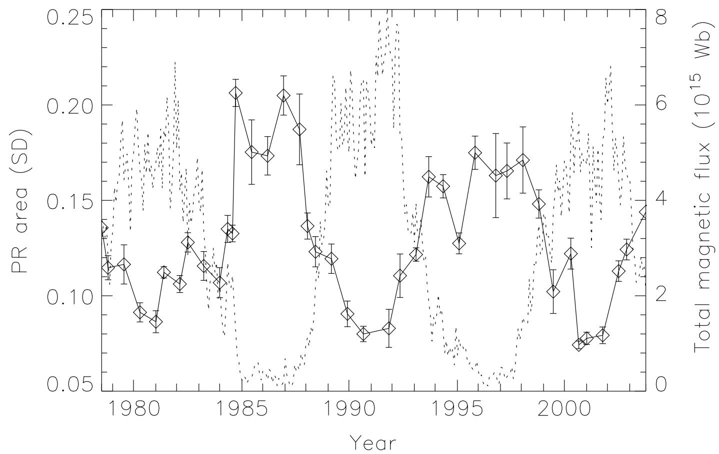

Fig. 2. PRs' area (solid) versus total unsigned magnetic flux sequence (dashed) during solar cycles 21 to 23. 1 SD means the area of whole solar disk.

we choose the time scale to keep its original Carrington coordinate on the consideration of most polar coronal holes having a rigid rotation. Second, we resize each latitudinal strip to a uniform dimension of 360 elements by a linear shrinkage or interpolation method. Then in the vertical direction we modulate the equal steps in sine latitude to equal steps in latitude to cut down the measurement errors near polar regions. Finally, a synoptic chart with a new grid is constructed, see figure 1b.

3 Analytical results

In reference to the result of Song & Wang (2006), we divide each hemisphere into four latitudinal zones, which represent the PR, the high-latitude region, the activity belt and the low-latitude region.

3.1 The polar region

For two PRs, because of an obvious projection effect in the measurement of magnetic field, we analyze the area instead of total magnetic flux. In order to identify PRs' boundaries in Kitt peak magnetograms, we set two criterions: (1) During solar minimums, both PRs are unipolar flux regions; (2) During solar maximums, the outer boundaries of plage regions can be regarded as those of PRs. The measurement result is displayed in figure 2 in which the time resolution is about 10 CRs and the average measurement error is about 7%. For making a good comparison we superpose the total unsigned magnetic flux (we measure it also using Kitt Peak charts and choose pixels with value

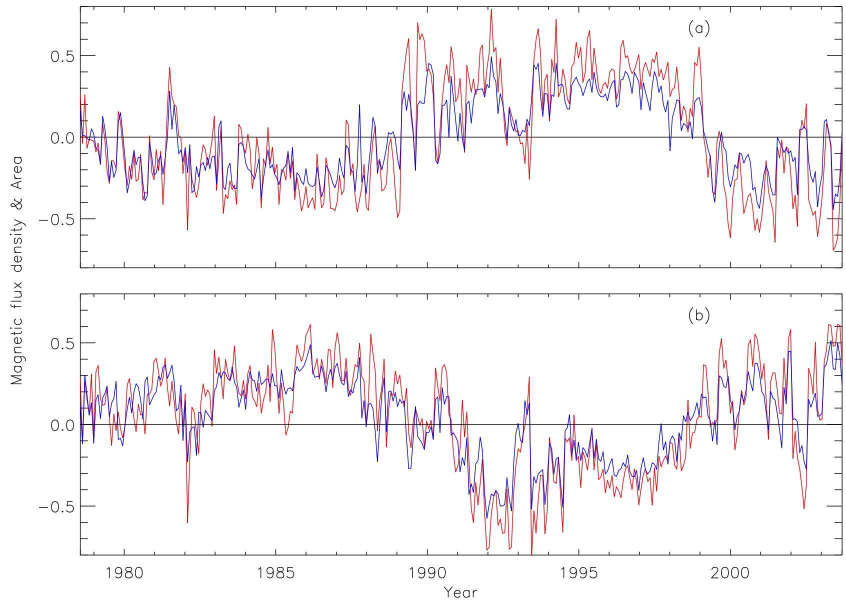

Fig. 3. The proportions of mean magnetic flux density (blue) and area (red) between two magnetic polarities in high-latitude regions. Panel a is for the northern hemisphere, panel b is for the southern hemisphere.

higher than 20 Gauss in the range of $|\theta| \leq 60°$) in it. It is obvious that PRs' area varies in completely anti-phase to the flux sequence. From their relative peak strengths we further find a coherence existing between the flux sequence and PRs' area with a time lag of 5 years. Makarov et al. (2003) find a similar relation using the duration of the polarity reversal in the octupole component of solar magnetic field. Such a correlation in strength may give evidence of solar cycle to be initiated from PRs just as described by Babcock (1961).

3.2 The high-latitude region

The borderline between the high-latitude region and the activity belt is chosen the position where $\theta = \pm 40°$. However sometimes we can meet several active regions located higher than this latitude, then the borderline will be adjusted to be a bit higher than these active regions. We mainly investigate two parameters in this region. They are $m = \frac{m_p - m_n}{m_p + m_n}$ and $a = \frac{a_p - a_n}{a_p + a_n}$, where m indicates the mean magnetic flux density, a indicates the area, p is for the positive magnetic flux and n is for the negative magnetic flux. The result is shown in figure 3. From it we can find such two parameters vary simultaneously and the high-latitude region always appear unipolar (the dominant polarity occupies more than 70%) except during a short time interval for the polarity reversal every other solar cycle. It is notable that the epochs when the polarity signs change is near the years of 1979, 1989 and 1999 which lag

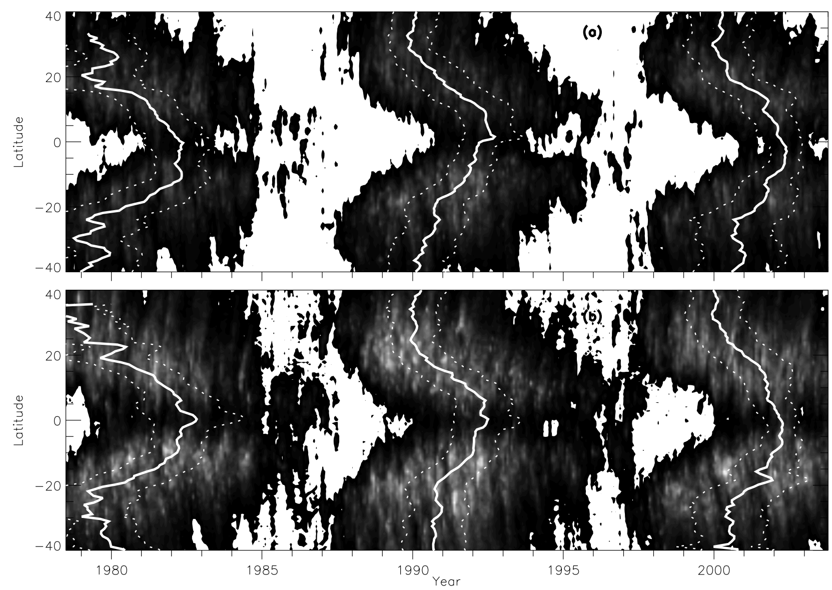

Fig. 4. Contours of average positive (a) and negative (b) magnetic flux density refer to the range of $|\theta| \leq 40°$. Six solid curves indicate the center positions of Gaussian fit and their side dashed lines indicate $\pm 1\sigma$ uncertainty estimates.

solar minimums for about 3 years. The main magnetic feature in high-latitude regions is plage which is usually and approximately coincide with faculae in the underlying photosphere. Sheeley (1991) finds a 90° phase shift between the number of polar faculae (it would be in a more extended polar region than ours defined in section 3.1) and the sunspot number, also with the sunspot number occurring earlier.

3.3 the activity belt and the low-latitude region

Figure 4 depicts the contours of average positive and negative magnetic flux density of all latitudinal strips (the strip width is 1°) refer to the range of $|\theta| \leq 40°$. A similar chart without the consideration of differential rotation is drawn by Dikpati et al. (2004). We find it is very like the butterfly diagram of sunspots. In order to analyze the flux peak time (or the main phase of solar cycle) in different latitudinal strips, we compute their Gaussian fits for every solar cycles. The Gaussian centers are described by six solid curves in figure 4 from which we can find that the variabilities of flux peak time exhibit two obvious inflexions near $\theta = \pm 20°$. In the higher latitude regions (or two activity belts) the flux peak time appears a bit steady which shows a good coherence with solar maximums. However, in the low-latitude regions the flux peak time starts to shift forward with an average gradient of 32.2 ± 12.4 day/deg.

4 Conclusion

According to the behaviors shown above, we find four typical solar latitudinal strips have different solar cycle phases. (1) The variability of PRs' area has a correlation with total unsigned magnetic flux in advance of 5 years. (2) The high-latitude region mainly appears unipolar in the whole solar cycle and its flux peak time lags sunspot cycle for 3 years. (3) For the activity belt, it is not surprised that its phase is the same as sunspot's. (4) The flux peak time of the low-latitude region shifts forward with an average gradient of 32.2 day/deg. Generally speaking, dynamo theory is developed for reproducing the well-regulated solar cycle. Here we propose the typical large-scale solar cycle features of solar magnetic field and they appear to be able to give some helps in constructing a more reliable solar dynamo.

References

Babcock, H.W., The topology of the sun's magnetic field and the 22-year cycle, 1961, ApJ, 133, 572-589

Dikpati, M., Solar magnetic fields and the dynamo theory, 2005, Advances in Space Research, 35, 322-328

Dikpati, M., de Toma, G., Gilman, P., et al., Diagnostics of polar field reversal in solar cycle 23 using a flux transport dynamo model, 2004, ApJ, 601, 1136-1151

Li, L.H., Sofia, S., & Belvedere, G., A flux tube solar dynamo model based on the competing role of buoyancy and downflows, 2005, ApJ, 629, 1164-1174

Makarov, V.I., Tlatov, A.G., & Sivaraman, K.R., Duration of polar activity cycles and their relation to sunspot activity, 2003, Sol. Phys., 214, 41-54

Parker, E.N., Hydromagnetic dynamo models, 1955, ApJ, 122, 293-314

Parker, E.N., Solar activity and classical physics, 2001, Chinese J. Astron. Astrophys., 1, 99-124

Sheeley, N.R., Jr., Polar faculae: 1906-1990, 1991, ApJ, 374, 386-389

Song, W., & Wang, J., The differential rotation and longitudinal distribution of solar magnetic flux, 2005, ApJ, 624, L137-140

Song, W., & Wang, J., Large-scale solar cycle features of photospheric magnetic flux, 2006, ApJ, 643, L69-72

Stenflo, J.O., & Güdel, M., Evolution of solar magnetic fields - modal structure, 1988, A&A, 191, 137-148